

Hocine Fekih\*, Boubakar Seddik Bouazza and Keltoum Nouri

# Performances of BICM-ID system using CRSC code in optical transmissions

<https://doi.org/10.1515/joc-2020-0073>

Received April 1, 2020; accepted August 17, 2020;

published online October 14, 2020

**Abstract:** Recently, using iterative decoding algorithms to achieve an interesting bit error rate for spectrally efficient modulation become a necessity for optical transmission, in this paper, we propose a coded modulation scheme based on bit interleaving circular recursive systematic convolutional (CRSC) code and 16-QAM modulation. The proposal system considered as a serial concatenation of a channel encoder, a bit interleaver and M-ary modulator can be flexible easy to implement using a short code length. For a spectral efficiency  $\eta = 3\text{bit/s/Hz}$ , the coding gain at a bit error rate of  $10^{-6}$  is about 8 dB.

**Keywords:** bit-interleaved coded modulation; code rate; CRSC code; iterative decoding; optical transmission; spectral efficiency.

## 1 Introduction

Telecommunication operators search to increase the number of users of their optical systems significantly. However, the fact that several forms of noise often limit the optical networks required the development and use of error correction techniques and advanced modulation formats [1].

Until the mid-1970s, coding and modulation techniques were treated as two independent and separate entities. Optimization of the coding did not give good results in certain types of modulation (modulation with 2 or 4 phase states) so Ungerboeck [2] arrived at a practical solution in 1982, which allows taking full advantage of the coding with modulations with an important number of states. The idea is to do the coding directly in the signal

space. The coding and modulation functions are no longer a single entity.

Zehavi [3] shows that the use of a bit interleaver can increase the order of diversity to the minimum number of distinct bits instead of channel symbols. This allows a coded modulation system of medium complexity to achieve a greater diversity order and reach a large gain of coding. This technique known as Bit-Interleaved Coded Modulation (BICM) [4].

Li and Ritcey [5] show during the year 1997 that it can improve the performances of BICM using iterative decoding (ID) especially after the introduction of the turbocodes in 1993 by Berrou et al. [6] because the performances of these codes are indeed very close to the theoretical limit of Shannon. Bit-Interleaved Coded Modulation with Iterative Decoding (BICM-ID) names this technique.

Djordjevic et al. and Milenkovic et al. [7, 8] show that the use of ID can improve bit error rate (BER) performance and decoder hardware complexity by using low-density parity-check (LDPC) codes for Wavelength Division Multiplexing (WDM) high-speed long-haul transmission. To improve this, Djordjevic et al. [9] have proposed an alternative technique for optical transmission using bit-interleaved LDPC-coded modulation (BI-LDPC-CM) and M-ary differential phase-shift keying (DPSK). In addition, the simulation results show that this technique can provide a significant coding gain.

Three years after the study by Djordjevic et al. [9], Arabaci et al. [10] have proposed a new scheme for coded modulation based on nonbinary quasicyclic low-density parity-check codes (NB-LDPC-CM) for optical transmission, and they show that using NB-LDPC-CM offers several advantages (decrease latency and the system complexity) in addition, the proposed scheme provides higher coding gains than BI-LDPC-CM [10].

The objective of this paper is to propose a BICM-ID system for optical transmission using a 16-state circular recursive systematic convolutional code (CRSC) and 16-QAM modulation. Optical wireless communications (OWCs) become part of our lives that can be employed in many ranges of communication applications from optical interconnects within integrated circuits through outdoor interbuilding links to satellite communications [11].

\*Corresponding author: Hocine Fekih, Technology Laboratory of Communication, University of Saïda Dr. Tahar Moulay, 20000, Saïda, Algeria, E-mail: [hocine1758@gmail.com](mailto:hocine1758@gmail.com). <https://orcid.org/0000-0002-6539-267X>

Boubakar Seddik Bouazza and Keltoum Nouri, Technology Laboratory of Communication, University of Saïda Dr. Tahar Moulay, 20000, Saïda, Algeria

We show that this scheme can improve the performance of the OWC system with different spectral efficiencies.

In this study, we will give the general structure of BICM system and a view of the recursive convolutional codes. We will discuss in more detail the BICM and BICM-ID systems. Next, we will give a description and an initialization of the parameters used in our system in order to evaluate the BER according to the signal-to-noise ratio (SNR). The conclusions are drawn in the final step.

## 2 Structure of the BICM-ID

Zehavi imagined the idea of BICM systems that are based on bit interleaving and he suggests a coded system built from a convolutional encoder followed by interleaver of random bits.

The convolutional code is a finite memory system that generates bits whenever information bits are presented at its input. However, unlike block codes, the output bits not only depend on the block of bits at the input of the encoder but also on the previous blocks. Convolutional codes thus introduce a memory effect of order; the quantity is called the constraint length of the code [12, 13]. Thus, the encoder consists of a stage register, which stores the last blocks of information bits, a combinatorial logic which calculates the blocks of bits supplied by the encoder and a parallel/serial converter. The general principle of convolutional coding is illustrated in Figure 1.

The conventional BICM system used in this study is built from a serial concatenation of a channel encoder, a bit interleaver and M-ary modulator, as shown in Figure 2. The information sequence is first coded by a convolutional encoder to provide coded sequences at its output [14].

The convolutional code must be chosen optimally to give a large Hamming free distance for a given code rate and constraint length. In this work, a convolutional code is

obtained from a natural code rate of the 16-state CRSC code and a generator polynomial (23, 35). The adoption of a circular code can guarantee that the initial state and the final state of the trellis are identical. The trellis then takes on the shape of a circle. In addition, the extremities of the block can benefit both from the past and from the future during the decoding process [15]. The pseudorandom interleaver swaps the encoded bits. It should be noted that we use only one-bit interleaver instead of the bit interleaver used in the Zehavi approach and this is for reasons of BICM flexibility and complexity of the analysis. After the interleaver, the interleaved coded bits are grouped as a symbol  $v=(v_1, \dots, v_2)$ , which is mapped to the complex signal  $x_t$  by a labeling function  $\mu$  with  $x_t=\mu(v)$ .

– The circular state:

At a point of time, the state  $S_i$  of the register is a function of the previous state  $S_{i-1}$  and of the previous input vector  $X_{i-1}$  [15]:

$$S_i = G \cdot S_{i-1} + X_{i-1} \quad (1)$$

where  $G$  is the generating matrix of the considered code. From Eq. (1), we can deduce:

$$S_i = G \cdot S_0 + X_0 \quad (2)$$

$S_i$  can be expressed as a function of the initial state and of the data supplied to the coder between instants 0 and  $i-1$ :

$$S_i = G^i S_0 + \sum_{p=1}^i G^{i-p} X_{p-1} \quad (3)$$

If  $k$  is the length of the sequence applied to the encoder input, the traffic state  $S_c$ , if it exists  $S_c = S_0 = S_k$ , or again:

$$S_c = G^k S_k + \sum_{p=1}^i G^{k-p} X_{p-1} \quad (4)$$

which give:

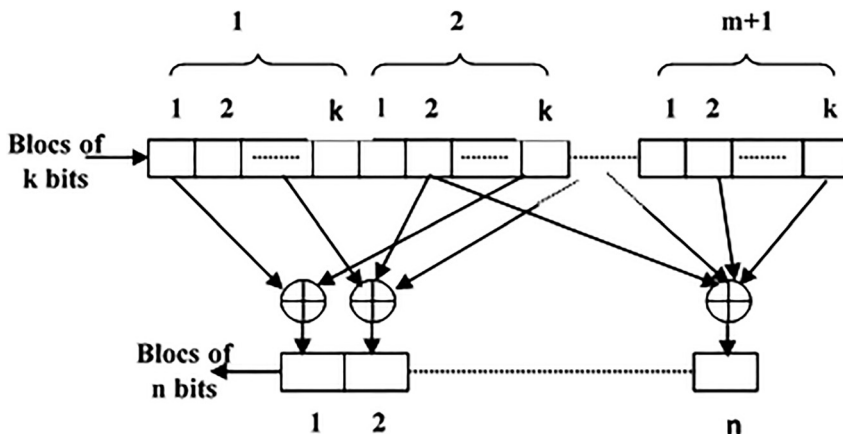


Figure 1: Convolutional code structure.

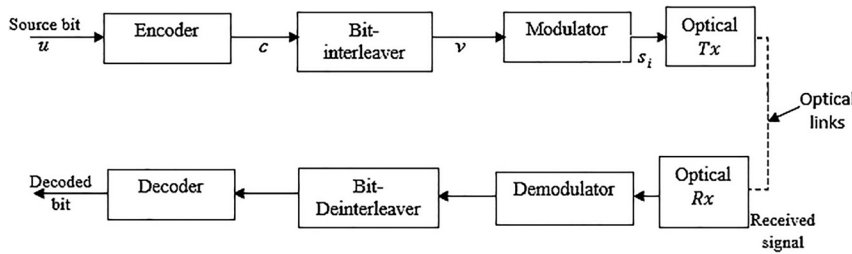


Figure 2: BICM scheme.

$$S_c = (I + G^k)^{-1} + \sum_{p=1}^i G^{k-p} X_{p-1} \quad (5)$$

If  $S_c$  exists, the encoder is initialized to the state  $S_c$ , it returns to this state when the data  $k$  has been encoded. The final state and the initial state can then be confused. The calculation of  $S_c$  requires preprocessing. The encoder is first initialized to the all-zero state and then the message to be encoded is transmitted to it. Using Eq. (5), the final state, noted  $S_k^0$ , can be written as:

$$S_k^0 = \sum_{p=1}^i G^{i-p} X_{p-1} \quad (6)$$

Using Eq. (6), the circular state can be calculated as follows:

$$S_c = (I + G^k)^{-1} S_k^0 \quad (7)$$

In practice, using a table makes it possible to determine  $S_c$  knowing  $S_k^0$  (Table 1).

To decode a convolutional code at the receiver side a maximum *a posteriori* probability (MAP) algorithm is used; we can calculate the posterior probability of each bit of information or of each transmitted symbol, and the corresponding decoder selects at each moment the most probable

bit or symbol. Bahl, Cocke, Jelinek and Raviv published this algorithm in 1974; the scope of this decoding method remained confidential until the implementation of turbo-codes [6] because it does not bring significant performance improvement over the Viterbi algorithm for decoding convolutional codes and is more complex to implement. On the other hand, the situation changed in 1993 because the decoding of turbo-codes makes use of elementary decoders with soft outputs as the MAP algorithm.

### 3 BICM-iterative decoding

To describe the iterative process of the BICM-ID system, we will take the case of a QPSK modulation, as shown in Figure 3.

The binary signal undergoes a convolutional encoder and through the random interleaver, after interleaving the coded bits are grouped as a symbol  $y'$ . The mapping function  $\mathbf{y} = \text{map}(\mathbf{y}')$  associates an integer value with a complex value  $\mathbf{y}$  according to the constellation used. Thus, the symbol is transmitted on a channel. On reception, the channel symbols are demodulated and dissociated by calculating the log of the likelihood ratio (LLR).

Table 1: Circular state values  $S_c$  for a 16-state.

N mod 15																$S_N^0$
	0	1	2	3	4	5	6	7	8	9	10	11	12	13	14	
1	0	14	3	13	7	9	4	10	15	1	12	2	8	6	11	5
2	0	11	13	6	10	1	7	12	5	14	8	3	15	4	2	9
3	0	8	9	1	2	10	11	3	4	12	13	5	6	14	15	7
4	0	3	4	7	8	11	12	15	1	2	5	6	9	10	13	14
5	0	12	5	9	11	7	14	2	6	10	3	15	13	1	8	4
6	0	4	12	8	9	13	5	1	2	6	14	10	11	15	7	3
7	0	6	10	12	5	3	15	9	11	13	1	7	14	8	4	2
8	0	7	8	15	1	6	9	14	3	4	11	12	2	5	10	13
9	0	5	14	11	13	8	3	6	10	15	4	1	7	2	9	12
10	0	13	7	10	15	2	8	5	14	3	9	4	1	12	6	11
11	0	2	6	4	12	14	10	8	9	11	15	13	5	7	3	1
12	0	9	11	2	6	15	13	4	12	5	7	14	10	3	1	8
13	0	10	15	5	14	4	1	11	13	7	2	8	3	9	12	6
14	0	15	1	14	3	12	2	13	7	8	6	9	4	11	5	10

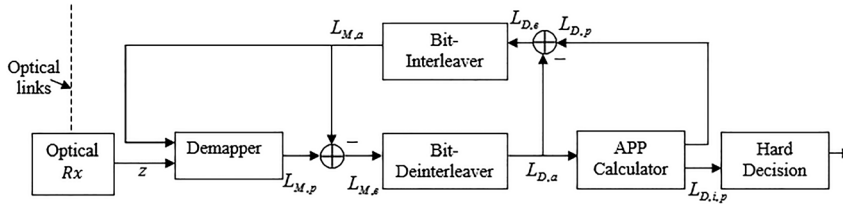


**Figure 3:** Iterative decoding scheme of a BICM-ID system.

After double deinterleaver, and soft-input/soft-output decoding (SISO) with a symbol per symbol calculator of posterior probability (APP), the estimates on the transmitted bits are available at the output of the hard decision process. This can be accomplished by a simple consideration of the sign of the value  $L_{D,i,p}$ , from APP to the output of the decoder.

In the iterative processing, the extrinsic information  $L_{D,e}$ , from the decoder is passed through the interleaver and returned to the soft process of demodulation as a prior knowledge  $L_{M,a}$ . The extrinsic information  $L_{D,e}$  at the level of the decoder is the difference between the input and output values of the LLRs on the coded bits,

$$L_{D,e} = L_{D,p} - L_{D,a} \quad (8)$$

The demodulator uses this extrinsic information from a decoder and calculates the values improved *a posteriori*  $L_{M,p}$ , which then go to the decoder for a next step in the iterative process.  $L_{M,e}$  is the difference of  $L$ -values *a posteriori* at the level of the demodulation process and forms the channel information and the extrinsic information.

$$L_{M,e} = L_{M,p} - L_{M,a} \quad (9)$$

For QPSK modulation, the demodulator needs to compute the log of the LLRs on the  $x_0$  and  $x_1$  coded bits for each symbol at the input. The  $L$ -value of the bit  $x_0$  conditioned at the output of the adapted filter can be calculated as follows:

$$L(x_0/z) = \ln \frac{\Pr(x_0 = 1|z)}{\Pr(x_0 = 0|z)} \quad (10)$$

$$= \ln \frac{\Pr(x_0 = 1, x_1 = 0|z) + \Pr(x_0 = 1, x_1 = 1|z)}{\Pr(x_0 = 0, x_1 = 0|z) + \Pr(x_0 = 0, x_1 = 1|z)} \quad (11)$$

## 4 System model

In this work, a convolutional code is obtained from a natural code rate  $R_c$  of the 16-state circular CRS code and a generator polynomial (23, 35). The modulations used are a 16-QAM modulation and the transmission takes place through an optical channel.

The optical transmission system suffers from different types of noises such as phase-induced intensity noise (PIIN), thermal noise, shot noise [16] and

interference noise [17], PIIN is eliminated [18], it is closely related to the MAI due to the overlapping of spectral from the different users [19, 20], In the context of OWCs, noise is considered to be a combination of major factors, shot noise and interference noise, the dominant source of noise is the receiver thermal noise, which can be modeled as additive and Gaussian [21]

$$\sigma^2 = \sigma_{sh}^2 + \sigma_{th}^2 + \sigma_{AWGN}^2 \quad (12)$$

$$\sigma_{sh}^2 = 2eIB \quad (13)$$

$$\sigma_{th}^2 = \frac{4K_b T_n B}{R_L} \quad (14)$$

the interference noise can be approximated as a Gaussian noise whose variance is proportional to the electrical signal power [21]. We assume this noise source is AWGN with zero mean and variance  $\sigma^2$  [22].

In the case of 16-QAM modulation, the variance is given by:

$$\sigma_{AWGN}^2 = \left( \frac{5}{4} \times 10^{-\frac{SNR}{10}} \right) \quad (15)$$

where  $T_n$  is the receiver temperature,  $R_L$  is the receiver resistance,  $B$  is the receiver electrical bandwidth and  $K_b$  is Boltzmann's constant.

The decoding used with a SISO MAP algorithm.

To initialize the trellis, we need a preliminary step called "prologue" and the following algorithm parameters.

### 4.1 Expression of the joint probability

$$\lambda_k^i(m) = P(d_k = i, S_k = m / R_1^N) \quad (16)$$

$$\begin{aligned} \lambda_k^i(m) &= P(R_1^{k-1} / d_k = i, S_k = m, R_k^N) \times P(R_{k+1}^N / d_k = i, S_k \\ &= m, R_k) \times \frac{P(d_k = i, S_k = m, R_k)}{P(R_1^N)} \end{aligned} \quad (17)$$

We will set the state metric forward in:

$$\alpha_k(m) = \Pr(R_1^{k-1} / d_k = i, S_k = m, R_k^N) \quad (18)$$

However, the event produced after the moment  $k$  does not influence the events that preceded them the previous equation is reduced to

$$\alpha_k(m) = \Pr(R_1^{k-1}/S_k = m) \quad (19)$$

$$= \sum_{m'=0}^{2^M-1} \sum_{j=0}^1 P(d_{k-1} = j, S_{k-1} = m', (R_1^{k-1}|S_k = m)) \quad (20)$$

$$= \sum_{m'=0}^{2^M-1} \sum_{j=0}^1 P((R_1^{k-2}|S_k = m), d_{k-1} = j, S_{k-1} = m', R_{k-1}) \times P(d_{k-1} = j, S_{k-1} = m', (R_{k-1}|S_k = m)) \quad (21)$$

With  $b(j, m) = S_{k-1}$

$$\alpha_k(m) = \sum_{j=0}^1 P((R_1^{k-2}|S_k = b(j, m))P(d_{k-1} = j, S_{k-1} = b(j, m), R_{k-1})) \quad (22)$$

$$\alpha_k(m) = \sum_{j=0}^1 \alpha_{k-1}(b(j, m)) \cdot \delta_{k-1}^j(b(j, m)) \quad (23)$$

In the same way, we also define the state metric backward:

$$\beta_k(m) = \Pr(R_k^N/S_k = m) \quad (24)$$

$$\beta_k(m) = \sum_{j=0}^1 \delta_k^j(m) \beta_{k+1}(f(j, m)) \quad (25)$$

We define the branch metric by:

$$\delta_k^i(m) = P(d_k = i, S_k = m, R_k) \quad (26)$$

$$\delta_k^i(m) = P(r_k^s/d_k = i, S_k = m) \times P(r_k^p/d_k = i, S_k = m) \times P(S_k = m/d_k = i) \times P(d_k = i) \quad (27)$$

The expression of the joint probability becomes:

$$\lambda_k^i(m) = \frac{\alpha_k(m) \times \Pr(R_{k+1}^N/d_k = i, S_k = m, R_k) \times \delta_k^i(m)}{\Pr(R_1^N)} \quad (28)$$

$$\lambda_k^i(m) = \frac{\alpha_k(m) \times \beta_{k+1}(f(i, m)) \times \delta_k^i(m)}{\Pr(R_1^N)} \quad (29)$$

With  $f(j, m) = S_{k+1}$

Finally, we get the expression of LLR:

$$LLR(d_k) = \log \left[ \frac{\sum_{m=0}^{2^M-1} \alpha_k(m) \times \beta_{k+1}(f(1, m)) \times \delta_k^1(m)}{\sum_{m=0}^{2^M-1} \alpha_k(m) \times \beta_{k+1}(f(0, m)) \times \delta_k^0(m)} \right] \quad (30)$$

To calculate the forward and backward state metrics and the branch metrics, we use Eqs. (23), (25) and (27), respectively. The initialization of  $\alpha$  and  $\beta$  is given by:

–  $s_0$  is the initial state of the encoder

$$\alpha_0(s_0) = 1, \alpha_0(s) = 0_{\forall s \neq s_0}$$

–  $s_k$  is the final state of the encoder

$$\beta_k(s_k) = 1, \beta_k(s) = 0_{\forall s \neq s_k}$$

–  $\delta_k^i(m) = P(r_k^s/d_k = i, S_k = m) \times P(r_k^p/d_k = i, S_k = m)$

$$\times P(S_k = m/d_k = i) \times P(d_k = i)$$

The mappings used for 16-QAM modulation are shown in Figure 4.

## 5 Simulation results

In order to study and analyze the performance of a coded modulation, we choose a 16-QAM modulation associated with a convolutional code. This is done by varying the parameters affecting the performance of the system thus designed. For Bit-Interleaved CRSC-Coded Modulation, the number of global iterations between the APP calculator and Demapper is three as in a study by Arabaci et al. [10] (Table 2).

The performance comparison of coded modulation based on CRSC code and uncoded system is shown in

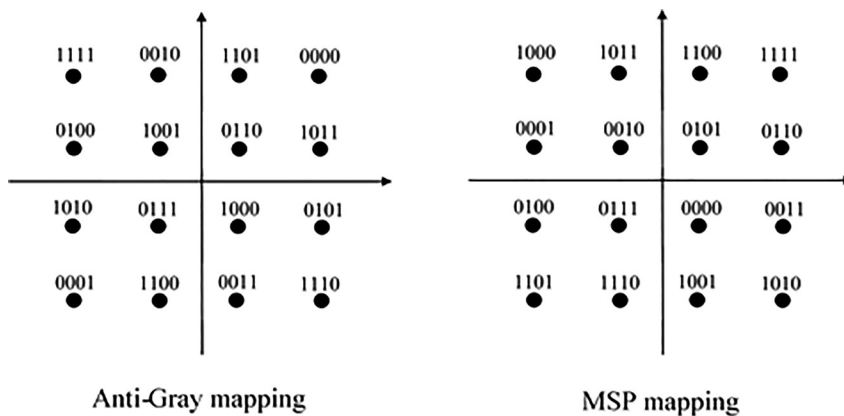


Figure 4: 16-QAM constellation with different mappings.



Table 2: Parameters used in simulation.

$\eta = 0.6$	Quantum efficiency.
$h = 6.62 \times 10^{-34}$	Plank's constant.
$P_{sr} = -10$ dbm	The effective power.
$B = 466.5$ MHz	Electrical bandwidth.
$R_L = 1030$	Receiver load resistor.
$K_b = 1.3806503 \times 10^{-23}$	Boltzman's constant.
$T_n = 300$ k	Receiver noise temperature.
$e = 1.6 \times 10^{-19}$ C	Electron's charge.
Bloc number = 500.	
Iteration number = 3	

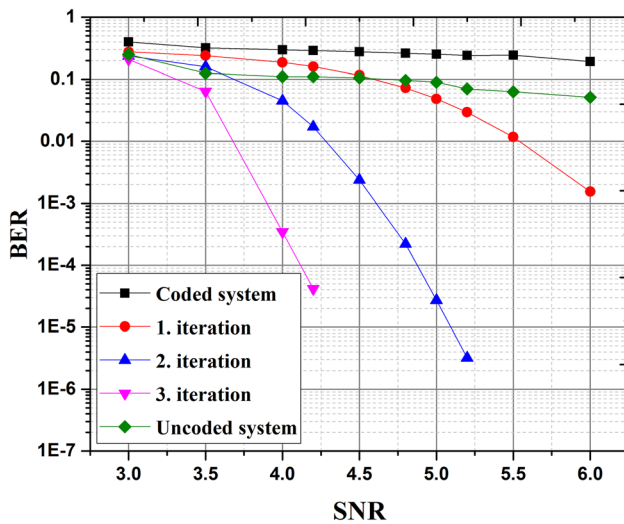


Figure 5: BER Performances of BICM-ID System Using CRSC Code with anti-Gray and mapping.

Figure 5. This figure shows a significantly better performance of a coded modulation (BICM) compared to uncoded modulation. In addition, Figure 5 shows that ID improves BICM performance.

To complete this study, we simulate the systems with two different mapping anti-Gray and Modified Set Partitioning (MSP) mapping. From Figure 6, we observe that the choice of the right mapping can achieve the targeted BER.

Now we simulate a Bit-Interleaved CRSC-Coded Modulation with IR with various code rates  $R_c = 3/4$  ( $\eta = 3$  bit/s/Hz), as illustrated in Figure 7.

From Figure 7, it is clear that channel coding improves BER performance. Note that the ID shows a good convergence threshold for low SNRs and that there is a coding gain of 8 dB between the coded system (third iteration) and uncoded system which leads to note the influence of using channel coding and ID in optical wireless networks.

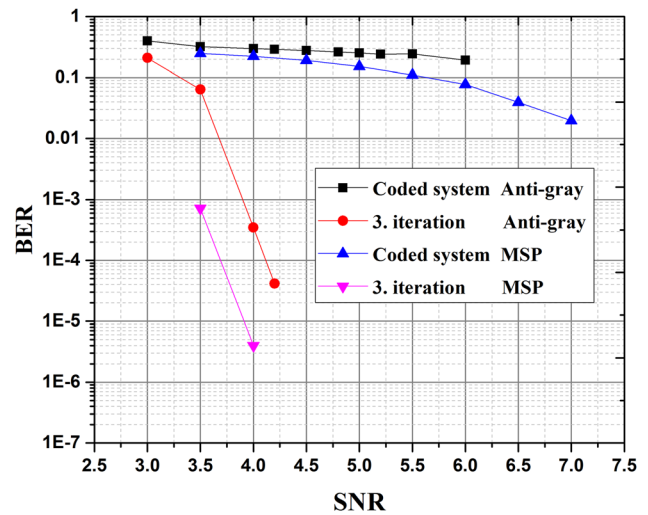


Figure 6: BER Performances of BICM-ID System Using different signal mappings.

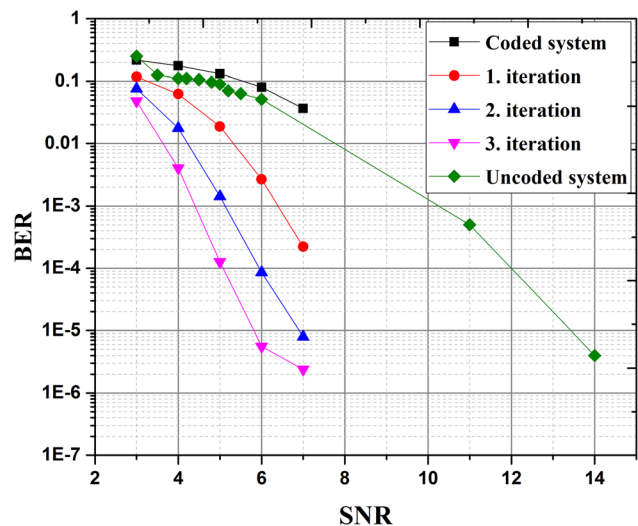


Figure 7: BER Performances of BICM-ID System with various code rates  $R_c = 3/4$  ( $\eta = 3$  bit/s/Hz).

## 6 Conclusion

In this article, we are particularly interested to study the performance of BICM-ID systems. The results of this comparative study using different parameters examined allow us to conclude that the performance of the BICM-ID system improves after each iteration, or a change in mapping. We can mention that the results obtained allow us to conclude that coded modulation makes it possible to design systems with high spectral efficiency.

Ultimately, this system built with a simple convolutional code has the advantage of being flexible and easy to implement. The selection of parameters depends on the application and system requirements.

**Author contribution:** All the authors have accepted responsibility for the entire content of this submitted manuscript and approved submission.

**Research funding:** None declared.

**Conflict of interest statement:** The authors declare no conflicts of interest regarding this article.

## References

1. Tzimpragos G, Kachris C, Djordjevic IB, Cvijetic M, Soudris D, Tomkos I. A survey on FEC codes for 100 G and beyond optical networks. *IEEE Commun Sur & Tutorials* 2014;18:209–21.
2. Ungerboeck G. Channel coding with multilevel/phase signals. *IEEE Trans Inf Theor* 1982;28:55–67.
3. Zehavi E. 8-PSK trellis codes for a fading channel. *IEEE Trans Commun* 1992;40:873–83.
4. Caire G, Taricco G, Biglieri E. Bit-interleaved coded modulation. *IEEE Trans Inf Theor* 1998;44:927–46.
5. Li X, Ritcey J. Bit-interleaved coded modulation with iterative decoding. *IEEE Commun Lett* 1997;1:169–71.
6. Berrou C, Glavieux A, Thitimajshima P. Near Shannon limit error-correcting coding and decoding: turbo-codes. 1. In: *Proceedings of ICC'93-IEEE International Conference on Communications*; 1993: IEEE. p. 1064–70.
7. Djordjevic IB, Sankaranarayanan S, Vasic BV. Projective-plane iteratively decodable block codes for WDM high-speed long-haul transmission systems. *J Lightwave Technol* 2004;22:695.
8. Milenkovic O, Djordjevic IB, Vasic B. Block-circulant low-density parity-check codes for optical communication systems. *IEEE J Sel Top Quant Electron* 2004;10:294–9.
9. Djordjevic IB, Cvijetic M, Xu L, Wang T. Proposal for beyond 100-Gb/s optical transmission based on bit-interleaved LDPC-coded modulation. *IEEE Photon Technol Lett* 2007;19:874–6.
10. Arabaci M, Djordjevic IB, Saunders R, Marcoccia RM. Nonbinary quasi-cyclic LDPC-based coded modulation for beyond 100-Gb/s transmission. *IEEE Photon Technol Lett* 2010;22:434–6.
11. Khalighi MA, Uysal M. Survey on free space optical communication: a communication theory perspective. *IEEE Commun Sur Tut* 2014;16:2231–58.
12. Hansen J, Ostergaard J, Kudahl J, Madsen JH. On Superregular Matrices and Convolutional Codes with Finite Decoder Memory. In: *2018 IEEE 87th Vehicular Technology Conference (VTC Spring)*. IEEE; 2018:1–5 p.
13. Viterbi AJ. An intuitive justification and a simplified implementation of the MAP decoder for convolutional codes. *IEEE J Sel Area Commun* 1998;16:260–4.
14. Bouazza BS, Djebbari A. Bit-interleaved coded modulation with iterative decoding using constellation shaping over Rayleigh fading channels. *AEU-Int J Elect Commun* 2007;61:405–10.
15. Berrou C, Douillard C, Jezequel M. Multiple parallel concatenation of circular recursive systematic convolutional (CRSC) codes des télécommunications. Springer; 1999: p. 166–72.
16. Bouarfa A, Kandouci M, Bojanic S. Enhanced performances of W/S SAC-OCDMA system using LDPC code. *J Opt Commun* 2022;43: 129–36.
17. Boucouvalas A. Indoor ambient light noise and its effect on wireless optical links. *IEE Proc – Optoelectron* 1996;143:334–8.
18. Cherifi A, Yagoubi B, Bouazza B, Dahman A. Performance analysis of optical CDMA system based on zero cross correlation (ZCC) code using OFDM modulation. *Int J Signal Process* 2016;1:91–6.
19. Garadi A, Bouazza BS, Bouarfa A, Meddah K. Enhanced performances of SAC-OCDMA system by using polarization encoding. *J Opt Commun* 2020;40:319–24.
20. Bouarfa A, Kandouci M, Djellab H. A new MIHP code using direct detection for SAC-OCDMA system. *Int J Elect Eng Inf* 2017;9: 825–33.
21. Narasimhan R, Audeh MD, Kahn JM. Effect of electronic-ballast fluorescent lighting on wireless infrared links. *IEE Proceedings-Optoelectronics* 1996;143:347–54.
22. Chaaban A, Hranilovic S. Capacity of optical wireless communication channels. *Philos Trans R Soc London Ser A* 2020; 378:20190184.